

Received December 8, 2020, accepted December 21, 2020, date of publication January 11, 2021, date of current version January 21, 2021.

Digital Object Identifier 10.1109/ACCESS.2021.3050877

A Generalised Methodology for the Diagnosis of Aircraft Systems

CORDELIA MATTUVARKUZHALI EZHILARASU¹, ZAKWAN SKAF, AND IAN K. JENNIONS²

¹Integrated Vehicle Health Management (IVHM) Centre, Cranfield University, Cranfield MK43 0AL, U.K.

Corresponding author: Cordelia Mattuvarkuzhali Ezhilarasu (c.m.ezhilarasu@cranfield.ac.uk)

This work was supported by Boeing Company, as part of their collaboration with Cranfield University IVHM Centre.

ABSTRACT An aircraft is made up of a number of complicated systems which work in harmony to ensure safe and trouble-free flight. In order to maintain such a platform, many diagnostic and prognostic techniques have been suggested, mostly aimed at components but some at the system level. Together these form a patchwork approach to the overall problem of efficiently informing aircraft maintenance to the Original Equipment Manufacturers, the operators /airlines, and the Maintenance, Repair, and Overhaul organisations. It involves these organisations having to support several different approaches to aircraft health management, and is therefore inefficient and costly. In the current work, a streamlined methodology is put forward. This is based on OSA-CBM (Open System Architecture for Condition Based Maintenance) and can be applied to any aircraft system. Integral with this is the use of mRMR (minimum redundancy maximum relevance) for feature selection, the resulting symptom vector being used for fault diagnosis. This approach is demonstrated on three test cases: the engine, the environmental control system, and the fuel system. In each case, the digital twin setup, simulation conditions for healthy and faulty scenarios, a methodology based on OSA-CBM up to diagnostics are detailed. Diagnostics is carried out for each system in turn, using four machine learning supervised algorithms. The best performing algorithm for each system will then subsequently be used in a vehicle level reasoner called FAVER (A Framework for Aerospace Vehicle Reasoning), which requires these system diagnoses as a starting point for vehicle reasoning and fault ambiguity resolution.

INDEX TERMS Aircraft systems, OSA-CBM, diagnosis, digital twin, minimum redundancy maximum relevance.

I. INTRODUCTION

An aircraft is a complex machine made up of multiple systems, as detailed by the FAA [1]. These systems are usually built-in isolation and assembled together on a common platform. Every aircraft system, such as the engine, the environmental control system (ECS), the fuel system, the electrical power system (EPS), the pneumatic system, or the auxiliary power unit (APU), has functions of its own and objectives to satisfy at different levels [2]. These objectives may range from the component level (e.g., the blade of a compressor in an engine), the line replaceable unit (LRU) level (e.g., gearbox assembly in an engine), the subsystem level (e.g., the engine compressor), the system level (e.g., the engine) or the overall vehicle level (the aircraft). One of the most important objectives of these aircraft systems, at any level, is to perform

safely at their optimal health and efficiency, contributing to the best performance of the aircraft, as well as saving the cost and time involved in maintenance, and unexpected downtime. In order to achieve this objective, Integrated Vehicle Health Management (IVHM) uses technology across numerous sources like sensor data, fleet history, maintenance records, and design documents to monitor and assess the health of the concerned asset (component/ LRU/ subsystem/ system/ vehicle), to diagnose any fault present in the asset and then to prognose its remaining useful life. In this way, IVHM capability enables aircraft Condition-Based Maintenance (CBM), resulting in the achievement of cost and time saving [3].

Currently, IVHM's principal focus is on components and LRUs, with subsystems and systems receiving less attention. For example, the Model-based Avionics Prognostic Reasoner provided a solution for non-intrusively monitoring the health and predicting remaining useful life for Electro Mechanical

The associate editor coordinating the review of this manuscript and approving it for publication was Yu Liu³.

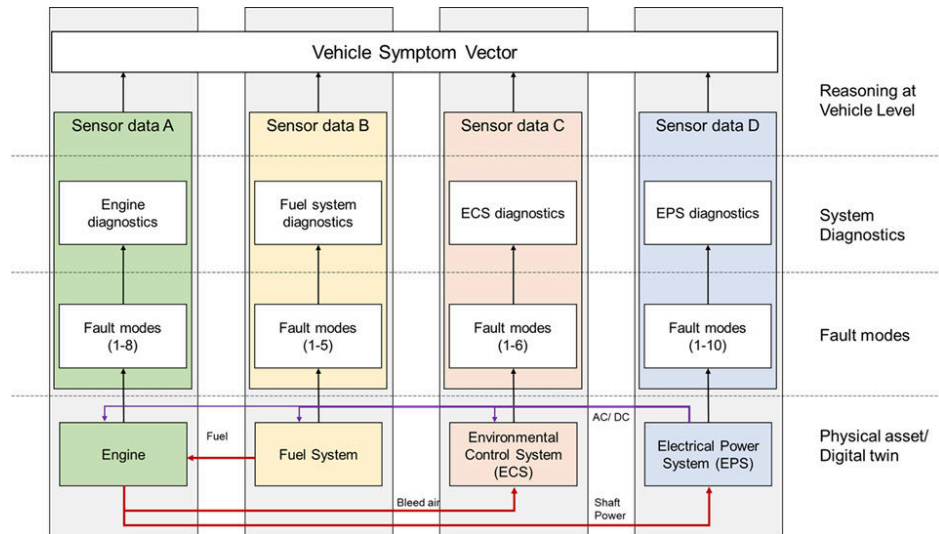


FIGURE 1. The schematic of FAVER.

Actuators by using exclusive algorithms and reasoning techniques [4]. Similarly, a high frequency vibration monitoring system was developed to detect and isolate incipient faults in critical rotary components in engines, gear trains, and generators. [5]. On the other hand, a framework based on symbolic dynamic filtering was developed to isolate faults in engine subsystems by interpreting and fusing data from multiple sensors in order to extract maximum information from the features [6]. These works show the extensive research carried out to isolate faults in components, LRUs, and subsystems in the aircraft.

However, none of these developments offers a rigorous process for the development of aircraft system diagnostics. A process that can effectively and efficiently inform aircraft maintenance to the OEM (Original Equipment Manufacturer) and the MRO (Maintenance, Repair, and Overhaul) organisations is needed. Such a system, based around OSA-CBM, is proposed here.

The idea for such an approach originated from a wider project named FAVER (Framework for Aerospace Vehicle Reasoning). The effect of the health state of one aircraft system over another due to their interactions, i.e., health assessment at the vehicle level, is not explored much in the technical literature, contributing to one of the significant gaps in the field of IVHM [7]. Aircraft accidents like the engine rollback incident on a Boeing 777 (2008) caused by a block in the fuel oil heat exchanger, and the emergency evacuation incident in a Fokker F28 (2002) caused by smoke in the cabin as a result of a crack in the APU compressor blade, are real life examples for multiple aircraft systems affected due to their interactions [2]. Isolating such cascading faults involves complex troubleshooting activities resulting in loss of time and increased cost due to extended downtime and prolonged maintenance. To address this gap, FAVER (fig 1) was proposed to isolate root causes and the effects

of cascading faults considering the health of multiple aircraft systems using the concepts of reasoning and digital twins [2]. In FAVER, there is a need for diagnostics built for each system under consideration, and hence the idea for generating such diagnostics in a rigorous manner emerged.

A. FAVER: A FRAMEWORK FOR AEROSPACE VEHICLE REASONING

While the concept of digital twins has been used across IVHM in a variety of roles [3], FAVER simulates multiple aircraft systems interacting with each other to demonstrate and isolate the effects of cascading faults at the vehicle level. Fig 1 shows the overall working mechanism of FAVER. As seen in the bottom row of fig 1, FAVER demonstrates the interaction between aircraft systems using digital twins and for the Electrical Power System (EPS), the engine, and the Environmental Control System (ECS), and hardware in the loop for the fuel system. The fuel system supplies fuel to the engine, the engine provides shaft power to the EPS and bleed air to the ECS, and the EPS provides electricity to the other three systems. Once the digital twin layer produces results for healthy conditions, and with certain fault modes, their health information is processed through diagnostics set up at the individual system level, as shown in the middle rows of fig 1. This is the subject of the current paper. Later, symptom vectors made from the health information from simulations of these individual digital twins, along with their diagnostic results, will be used by FAVER's reasoning as shown in the top row of fig 1, to identify the root cause and the effects on the interacting systems at the vehicle level.

B. THE NEED FOR A GENERALISED METHODOLOGY FOR THE DIAGNOSTIC PROCESS

Across the industry, maintenance of aircraft is mostly done by the OEMs or MROs. The format of health data acquired from

aircraft systems and the techniques applied by those carrying out, and troubleshooting, maintenance will vary considerably from platform to platform due to a lack of standardisation and development.

The functioning of IVHM systems at the systems level is not affected by the differences in the way health data is processed. However, in the case of a platform reasoner such as FAVER, since the reasoning is done at the overall aircraft level, processing data and carrying out the diagnosis for all concerned aircraft systems becomes complicated and tedious, especially when they are done using different methodologies.

Hence, there is a need to implement a generalised methodology to identify and streamline the repetitive steps involved in the diagnostic process. This will help save time spent in developing diagnoses for each aircraft system and make the overall aircraft level health reasoning faster and more practicable; to serve this purpose, the Open Systems Architecture for Condition-Based Maintenance (OSA-CBM) framework is employed.

This article demonstrates the application and usefulness of OSA-CBM as a generalised methodology for developing diagnostics for different aircraft systems. Section II focuses on the OSA-CBM methodology, and the steps involved in the process. Section III demonstrates the role of the OSA-CBM methodology through three different aircraft system use cases: the engine, the ECS, and the fuel system. Section IV provides the diagnosis part of these use cases, and Section V summarises the article and discusses ideas for future work.

II. THE OSA-CBM METHODOLOGY

OSA-CBM was developed in 2001 by an industrial team partially funded through a Dual Use Science and Technology (DUST) program [8]. Its aim was to define and develop open standards for distributed CBM. OSA-CBM implements ISO 13374 [9], Condition Monitoring and Diagnostics of Machines, to define the open standard. This standard breaks down the data collection, processing, and information flow into the six layers shown in fig 2. It defines the interfaces (data structure and interface methods) between each step and so, indirectly, what can happen in each of the layers [10]. Each layer is briefly described here.

Data Acquisition: Data is acquired from the target asset using sensors and other measuring devices, historical data, maintenance records, design documents, and other relevant information.

Data Manipulation: The collected data is preprocessed and made useful for further processing. This step could use feature extraction and feature selection processes.

State Detection: The processed data is used to monitor the current condition of the asset. This is done by comparing features against expected values, or operational limits and outputs enumerated condition indicators (e.g. low, normal, and high).

Health Assessment: This stage determines if the health of a monitored system or subsystem is degraded. Several types of diagnostic algorithms, such as model-based, data-driven,

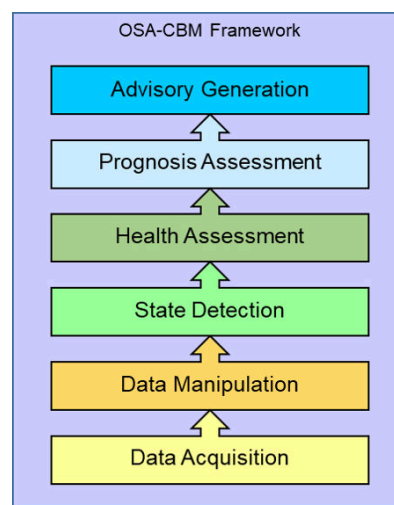


FIGURE 2. The Open Standard Architecture - Condition Based Maintenance (OSA-CBM) framework.

or hybrid algorithms, are used to assess the health of the asset. This layer generates a diagnostic record that proposes one or more possible fault conditions with associated confidence.

Prognostic Assessment: The remaining useful life and the future performance of the asset are then projected based on its state estimation results. In some cases, uncertainty propagation is also estimated using prognostic algorithms.

Advice Generation: Provide recommended actions and alternatives. Depending upon the applications, recommendations may include maintenance action schedules, modifying the operational configuration, or modifying mission profiles.

Because OSA-CBM is a standard and is not an instantiation of that standard, the above layer descriptions are open to interpretation and are given here for general guidance. OSA-CBM is defined using unified modelling language (UML), and is designed to enable multiple types of information to be processed without involving the technical interfaces. The OSA-CBM methodology can be applied at any stage of CBM, ranging from real-time health monitoring to portable maintenance and cloud services [8].

So far, in IVHM systems, the OSA-CBM framework steps are applied at the component, subsystem, and at the systems level. For example, at the LRU level, GE Aviation demonstrated the benefits of an IVHM system by monitoring the health state of an electromechanical actuator with parameters like the Hall effect sensor and supply current [11]. At the higher subsystem level, Boeing, the Air Force research laboratories, and Smith Aerospace together developed a program called Aircraft Electrical power systems Prognostics and Health Management and demonstrated health management of several subsystems for electrical actuation, fuel pump/valves, and arc fault protection by monitoring parameters like torque efficiency, motor performance, and vibration analysis [12]. At the systems level, Safran has developed an Engine Health Management program by monitoring multiple parameters such as oil consumption monitoring, oil and fuel filters

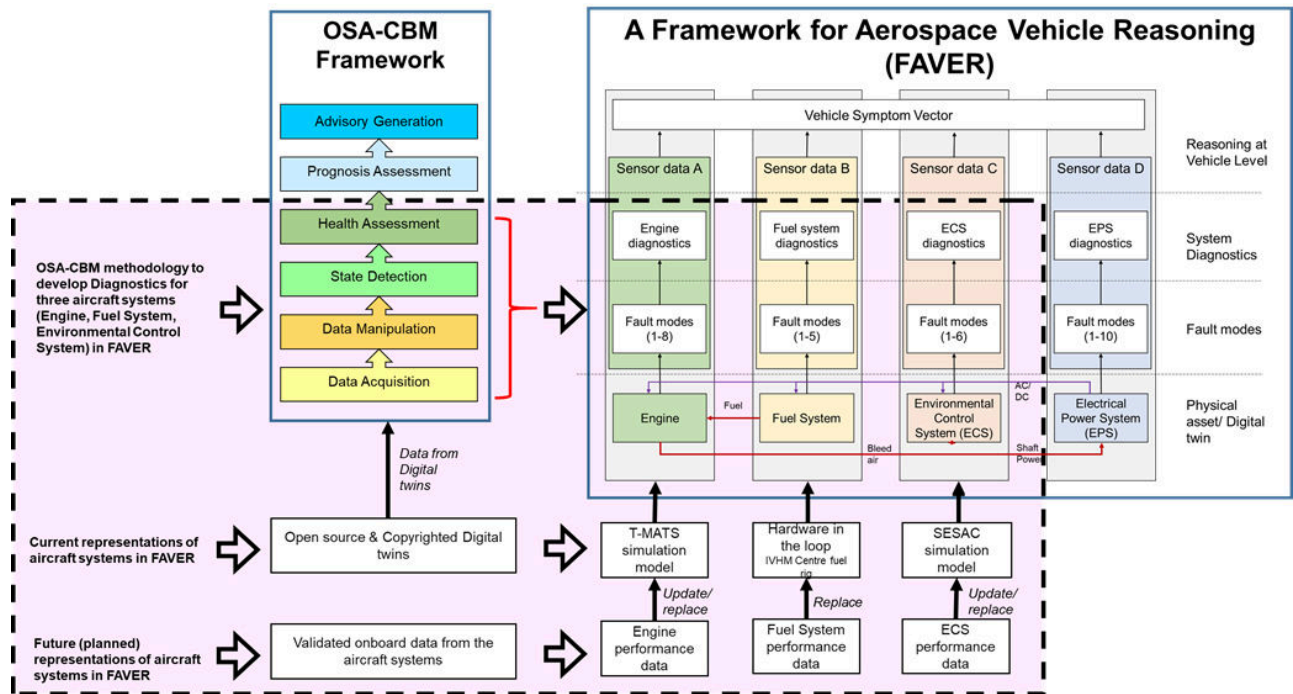


FIGURE 3. OSA-CBM methodology to develop diagnostics for three aircraft systems for a Framework for Aerospace Vehicle Reasoning (FAVER).

monitoring, actuation control loop monitoring, bearings vibration monitoring, and global performance monitoring [13]. Few more examples of applications of OSA-CBM can be found in these references ([14]–[16]). It can be seen from the examples that the aircraft systems have multiple sensors for multiple fault modes linked to multiple diagnostic algorithms. In this article, instead of following different processes for each aircraft system, a common methodology is sought and the series of steps from the OSA-CBM framework, leading up to health assessment (i.e., diagnosis), will be implemented for all concerned aircraft systems. The last two steps in the framework, viz, Prognostic Assessment and Advisory Generation, are not used in this article, as the goal is mainly to develop diagnostics. However, the results produced from diagnostics developed in this article for the aircraft systems, i.e., the symptom vectors, can be used for further prognostic assessment to provide maintenance solutions in practice.

A. CONTRIBUTIONS IN THIS PAPER

The work carried out in this article is shown in fig 3, highlighted by dotted black lines. In this work, three aircraft systems shown in the schematic diagram of FAVER (right side of fig 3) are examined: the engine, the ECS, and the fuel system. Previously, a simulation model of the EPS (Electrical Power System) was developed, with an Adaptive Neuro-Fuzzy Inference System (ANFIS) being implemented for its diagnosis [17]. It fits into the current framework but will not be replicated here. Diagnostics developed for these four aircraft systems are later used for vehicle level reasoning

in the platform level reasoner, FAVER, which is not covered in this article.

In this article, the following contributions are made with regard to these three aircraft systems:

- i) As seen in fig 3, the engine and the ECS digital twins are represented by MATLAB simulation models, while the fuel system is represented by hardware-in-the-loop (HIL), to show the flexibility of this approach. These models are run for healthy scenarios, and a certain number of faults are injected (both local and interacting faults), and their data recorded. In these digital twins, the simulation models are to be replaced by real performance data at the later stage, to represent the living models of the aircraft systems (as shown in the bottom part of fig 3).
- ii) Adhering to the OSA-CBM methodology (left part of fig 3), data from the digital twins is processed, and a feature selection algorithm (mRMR) is applied on all these systems to narrow down the health parameters necessary for developing the symptom vector as an input for the diagnosis.
- iii) The State Detection and Health Assessment steps of OSA-CBM are fused into one step by considering the diagnosis of faults as a classification problem. Here, the classification will take care of both, detecting if the symptom vector is healthy or faulty. In the case of a faulty symptom vector, the classification algorithm will also diagnose the fault. As mentioned previously, the developed diagnostics are to be used later in FAVER for vehicle level reasoning.

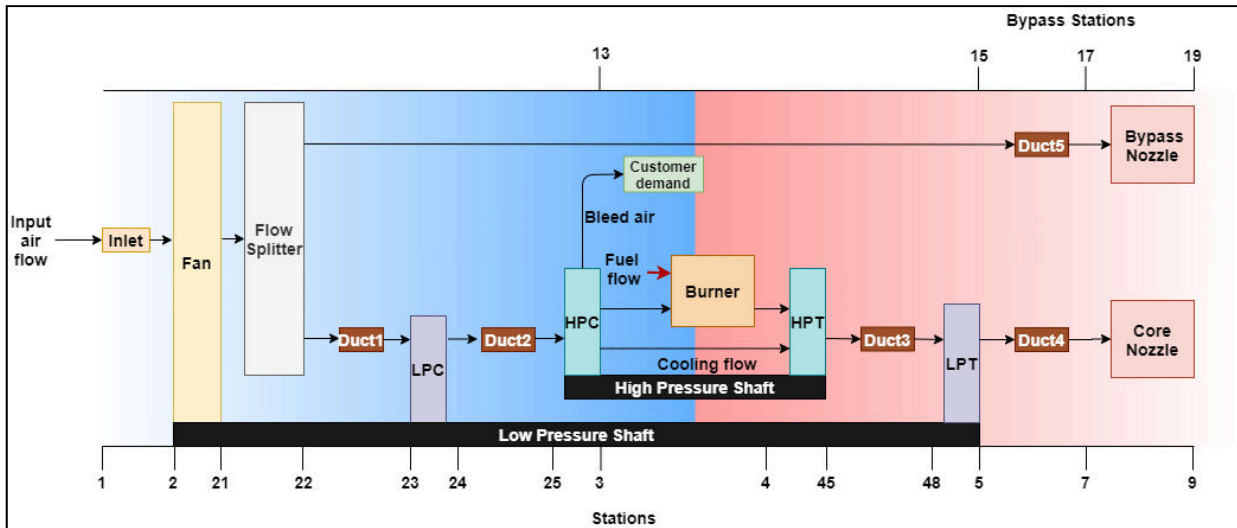


FIGURE 4. Turbofan engine block model in T-MATS (adapted from [20]).

The diagnostics for all three aircraft systems follow the data-driven approach in order to maintain uniformity and save time. Only single faults are injected; simultaneous or multiple faults are not considered [2]. It is to be noted that these aircraft systems are represented by a combination of digital twins and HIL and are chosen as a part of the project, FAVER [2]. Diagnostics for any other aircraft system represented by different types of simulation models could also be developed using the OSA-CBM methodology.

III. USE CASES

This section presents the setup of system level diagnostics for three aircraft systems: the engine, the environmental control system (ECS), and the fuel system. These have been chosen to demonstrate the use of the OSA-CBM methodology and for their fit into the overall FAVER architecture.

A. THE ENGINE

The engine is a primary safety critical aircraft system. It produces thrust, powers the EPS, and provides bleed air required for anti-icing and the ECS of the aircraft. Among the types of jet engines, the turbofan is the most used by the civil airliners, as it optimises fuel consumption for the thrust produced. Fig 4 shows a block diagram of a high bypass turbofan engine. The turbofan engine is made up of the following standard components: fan, compressor, combustion chamber, turbine, and nozzle. The engine sucks air through the fan (stations 2-21 from fig 4), and a portion of it is ducted into the core (station 23), while the rest of the air is bypassed (station 13) through the flow splitter to the bypass nozzle (station 19). The core flow is then compressed (stations 23-3) before being sent to the combustion chamber (stations 3-4), where the compressed air is mixed with fuel and burnt, producing hot gases and increasing the temperature. The hot air then expands across the turbine blades (stations 4-5) and

then passes through the core nozzle (stations 7-9). The cold bypassed air passes through a similar nozzle (stations 17-19) and mixes with the core flow to produce the thrust that moves the aircraft forward [18]. Bleed air is extracted from the compressor (station 3) based on demand, and supplied to the ECS and for anti-icing and deicing.

1) DIGITAL TWIN SETUP

The model chosen for the engine digital twin is the Pratt & Whitney JT9D open source turbofan engine model provided by T-MATS software in MATLAB Simulink [19]. This model features a high bypass turbofan engine with a bypass ratio of 4.8:1, one stage fan, three stage Low Pressure Compressor (LPC), 11 stage High Pressure Compressor (HPC), annular combustion chamber, two stage High Pressure Turbine (HPT), four stage Low Pressure Turbine (LPT), and a convergent divergent nozzle.

The healthy scenario is run with input conditions of 34000 ft altitude, 0.8 Mach number, and 1.91 pounds per second (pps) fuel mass flow rate, along with the efficiencies set as default in T-MATS [20]. A total of eight fault modes, including local and interacting faults, are simulated in T-MATS for this article, by reducing the efficiency of the subsystems as well as introducing leakages and blockages in the ducts and valves. The efficiency degradation and the leak induced in the fault modes are randomly chosen, and hence the resulting engine performance for each degradation mode can be viewed for the trend but not cross-compared for quantitative effect. For brevity in this engine simulation, only one mode of degradation is simulated for each subsystem. This single mode of degradation for each fault is sufficient for demonstrating the approach advocated here; the diagnostics could always be updated with multiple degradations and different fault modes at a later date. The following are the eight

selected faults injected in this simulation model; the first five are local faults, and the last three are interacting faults.

Local Faults: These engine faults do not affect other aircraft systems. However, as a result of these fault modes, the subsystems function with reduced efficiency, contributing to overall reduced efficiency for the engine.

- i) **Fan FOD:** Foreign Object Damage in fan blade reducing the efficiency of the fan by 2.7%
- ii) **LPC Contamination:** Blade corrosion in LPC reducing the efficiency of LPC by 3%
- iii) **HPC Fouling:** Fouling in HPC reducing the efficiency of HPC by 1.1%
- iv) **HPT Blade Broken:** Partial loss of blade in HPT reducing the efficiency of HPT by 1%
- v) **LPT Blade Broken:** Partial loss of blade in LPT reducing the efficiency of LPT by 3%

Interacting Faults: These faults are either caused by, or affect aircraft systems other than the engine.

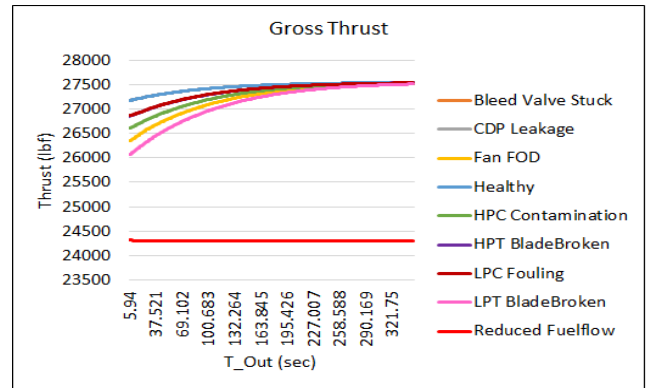
- vi) **Bleed Valve Stuck:** The bleed valve is stuck at 60 degrees. This fault affects the engine indirectly but directly affects the bleed air supplied to the ECS.
- vii) **CDP Leakage:** This fault is due to a 0.5% leakage in the duct carrying the bleed air from the engine to the ECS. Similar to the previous fault, this fault has the potential to affect the bleed air supplied to the ECS but does not affect the engine directly.
- viii) **Reduced Fuel flow:** The input fuel flow is reduced by 10%, a fault that could have been caused by a reduction of fuel pump speed. The reduced fuel input affects the engine performance directly.

The simulation model is adapted to include a simple Proportional Integrator (PI) controller, which is programmed to meet the demanded thrust as the overall objective. This is achieved by calculating Thrust Specific Fuel Consumption (TSFC) as shown in (1):

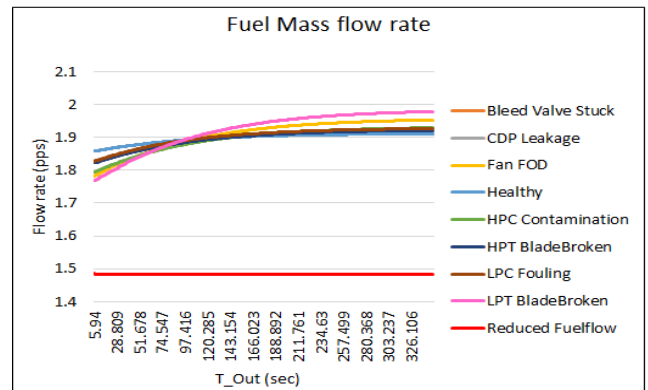
$$TFSC = \frac{m}{f} \tag{1}$$

where, m is the fuel mass flow rate, and f is the gross thrust. TSFC is provided as feedback to the PI controller, where the input fuel flow is altered by the controller to achieve the demanded thrust. As can be seen from fig 5(a), for all fault modes except **Reduced Fuel flow**, the demanded thrust objective (27500 lbf) is met, which is due to the PI controller. In the case of the **Reduced Fuel flow** fault mode, the loss of mass flow rate affects the gross thrust, as they are directly proportional to each other, as shown in (1). This can also be seen in fig 5(b), where the mass flow rate of the fuel increases in fault modes in order to achieve the thrust, except for the **Reduced Fuel flow** fault mode where the mass flow stays constant and hence does not achieve the demanded thrust.

Parameters like flow, total temperature, total pressure, enthalpy, and fuel-air ratio are measured at several stations, along with other parameters such as fan speed, core speed, torque, and TFSC. The data collected from the simulations



(a) Engine achieving the objective of demanded thrust for simulations of healthy (sky blue colour) and faulty scenarios. Reduced Fuelflow (red colour) mode could not achieve the demanded thrust.



(b) Fuel flow rate in healthy (sky blue colour) and faulty scenarios. Note that the flow rate increases in fault modes to achieve the demanded thrust. Reduced Fuelflow (red colour) mode could not achieve the demanded thrust.

FIGURE 5. Gross thrust and fuel flow rate in healthy and faulty scenarios.

are then used for developing further diagnostics for the failure modes mentioned in this section.

2) DATA ACQUISITION AND DATA MANIPULATION

The engine digital twin conFig in T-MATS is run in MATLAB R2019b for both healthy and faulty scenarios until the objective of thrust demanded is reached.

The next step is data manipulation, where the raw data collected from the simulations are formatted in MS EXCEL for further process in the OSA-CBM methodology. Only steady state data are used in the process; the rest of the data are ignored. Further, the number of health parameters to be monitored are narrowed down only to the essential features. This is because many parameters extracted from the simulation would be redundant to each other; hence monitoring all parameters from the simulation results would be time-consuming as well as would require higher processing power. In order to avoid this issue, feature analysis for each simulation model is carried out, and only the most influencing features are chosen for condition monitoring and diagnosis of the system.

Health parameters like flow, enthalpy, temperature, pressure, fuel-air ratio, are measured at several stations along

the gas flow path, with other calculated measures like thrust, TSFC, core speed, fan speed, and torque. Additional measurements are made near the bleed valve, which does not fall under the gas flow path. These result in a total of 85 features from which data is extracted to monitor the performance of the engine. In order to save time and reduce the complexity of the monitoring process, only the important features that influence or represent the engine performance are selected for the diagnostic process. This is carried out in two steps.

Step 1: Only the ‘measurements’ from the Digital Twin that would correspond to sensors in a real engine, such as temperature (Tt), pressure (Pt), mass flow (Wf), speed, TSFC, and thrust, are chosen. This results in 35 features.

Step 2: From the 35 features, the second stage of selection is carried out using the Minimum Redundancy Maximum Relevance (mRMR) algorithm. The mRMR algorithm is a selection algorithm that finds the optimal set of features with respect to the response variable by identifying the features with maximal and mutually dissimilar relevance and with minimal redundancy. This is done by calculating the mutual information between features and the response variable and through pair wise comparison of features itself [21].

In general, mutual information MI between two variables S,T is given by (2). This helps in finding how the variable S is helpful in reducing the uncertainty of variable T.

$$MI(S, T) = \sum_{ij} P(S = s_i, T = t_j) \times \log \left(\frac{P(S = s_i, T = t_j)}{P(S = s_i) P(T = t_j)} \right) \quad (2)$$

The mutual information is calculated for mRMR algorithm in the following fashion. Consider an empty set G , representing the optimal set of features ($G = \{\}$). Let H be the set containing the features, x, z ($H = \{x, z\}$), and let y be the response variable. The mRMR algorithm aims to add suitable features to the set G from set H . It does so by choosing the feature x (from set H) with maximum relevance (P_x), with respect to the response variable y , as calculated by (3) and assigning it to set G . In the next step, the feature z from set H is compared with x from set G , to minimise the redundancy by calculating (Q_x) between through (4). The mutual information quotient (MIQ) is then calculated using (5) and is used to rank all features in set G [22]:

$$P_x = MI(x, y) \quad (3)$$

$$Q_x = \left(\frac{1}{|G|} \right) \sum_{z \in G} MI(x, z) \quad (4)$$

$$MIQ = \frac{P_x}{Q_x} \quad (5)$$

$|G|$ is the number of features in set G . Once the ranks are assigned for all the features in set H , the optimal set G is filled with features that have maximum MIQ. In MATLAB R2019b, the importance of the feature is quantified by calculating its score. The score is the ratio of the difference between the MI of the target and the considered feature to the

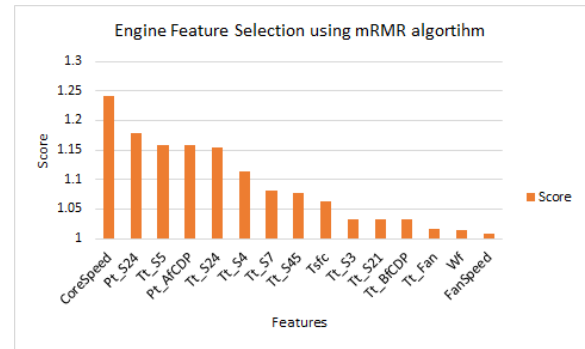


FIGURE 6. Top 15 features selected by mRMR algorithm for state detection and diagnosis of the engine.

average of MI of target and previously considered features. In short, the score represents the importance of the target feature with respect to the previously considered feature. The higher score for a feature indicates the importance of the predicting factor with respect to the response variable. The bigger difference in scores between the features shows the confidence of the algorithm in choosing one feature over the other [22].

While the ranks of features show exclusivity of the features using mutual information, the scores show their importance as predictors with respect to the response variables. In the case of engine simulation, the set H contains the 35 features, and set G will be populated with the features having higher ranks. This is done by calculating MI for all 35 features with respect to the response variable, i.e., the fault classes. This step will calculate the relevance of these features for better representation of the fault classes. Similarly, MI is calculated for pairwise comparison of these 35 features and measures the redundancy of these features. MIQ of these 35 features are then calculated and set G is populated with features having maximum MIQ, i.e., better ranks. In this step, the features which are least relevant are ranked the lowest. Finally, the scores of these ranked features are calculated by comparing the MI of each of these 35 features with respect to the average of the rest. Fig 6 shows the top 15 scored features and their ranks as calculated by the mRMR algorithm.

The final list of features required for condition monitoring and diagnosis of the engine is narrowed down based on the scores from 35 to only four, viz: i) Core speed (HP shaft speed), ii) Pressure at LPC exit (station 24): Pt_S24, iii) temperature at LPT exit (station 5): Tt_S5, and iv) pressure at the exit of bleed air duct: Pt_AfCDP.

Fig 6 shows the core speed and Pt_S24 possess the top-most scores among the monitored features. This indicates that these two features are better predictors of the engine health performance. This can be correlated with fig 7 (a) and fig 7 (b), where the features, core speed, and Pt_S24 show clear distinction among different fault modes from the healthy case of the engine. (Only steady state is considered in this simulation. Hence, in fig 7, data from $t = 230s$ is chosen for

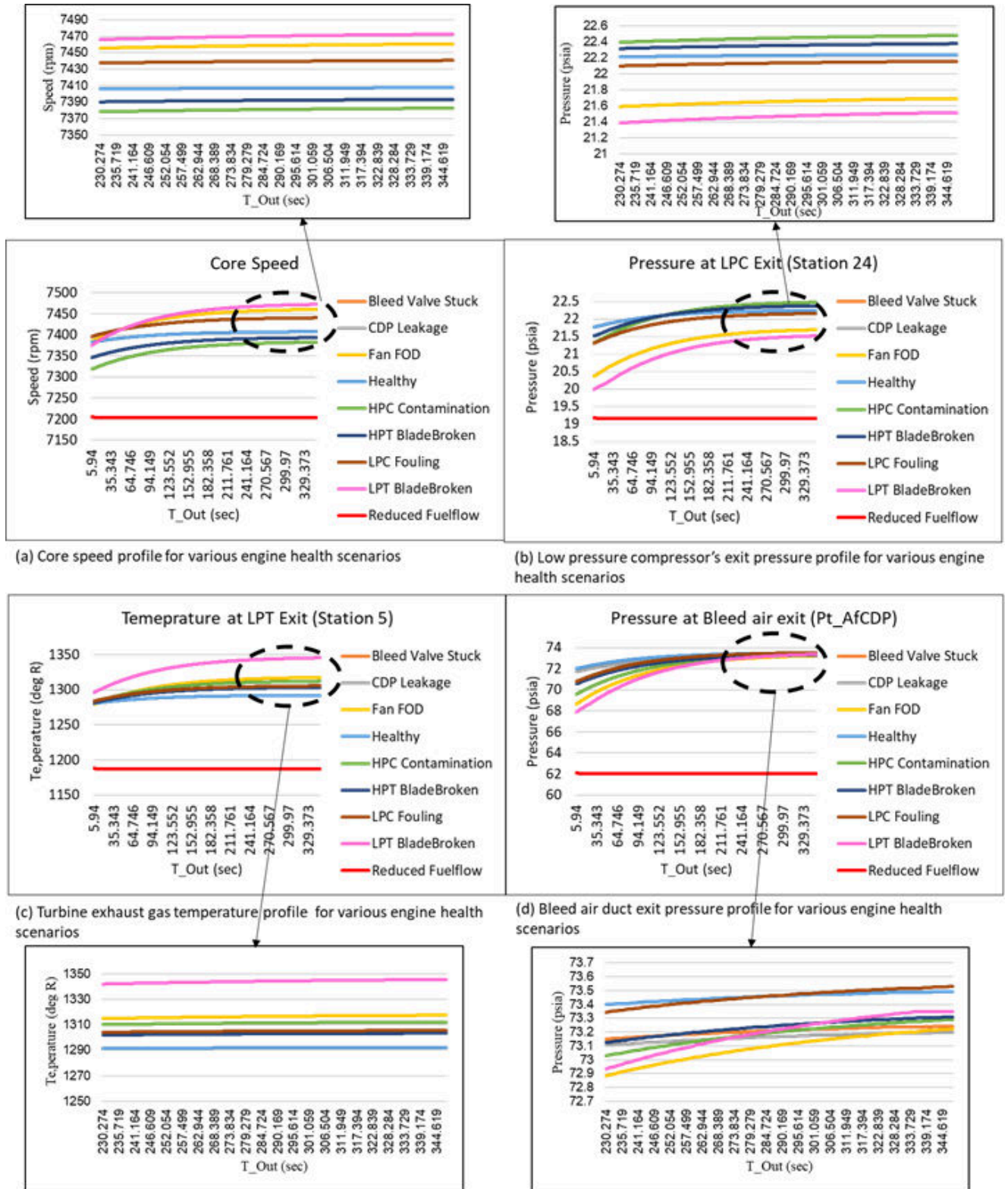


FIGURE 7. Performance of engine features for healthy and faulty scenarios.

analysis and interpretation. The entire timeline from $t = 0$ is shown in fig 7 for clarity). The turbine exit gas temperature

from fig 6, $T_{t,S5}$, has a better score, and can understandably predict the health of the engine (as seen in fig 7(c)), because of

its location in the gas path. As corroborating evidence, across the literature, these three features are proven predictors of engine health performance [23]–[25].

The strength of the mRMR algorithm is demonstrated in choosing the Pt_AfCDP feature in fig 6. Identifying the importance of Pt_AfCDP would not be normally possible without the help of the mRMR algorithm, as this feature is not directly related to any of the stations in the engine model, not located in the gas path of the engine, and was placed only to measure the exit pressure in the bleed air system ducts. However, the pressure sensor placement has resulted in this feature Pt_AfCDP to function as a predictor of the engine health. This can be observed from fig 7(d), where the pressure at the bleed air exit has a distinct profile for each fault mode and is differentiated clearly from the healthy case. Thus, the mRMR algorithm has successfully selected the most important predictors of the engine health performance as well as aided the selection of optimal sensor placement for monitoring the engine health. The next step is to use these four features to detect the current state of the engine and to diagnose fault modes.

3) STATE DETECTION

In the state detection step of OSA-CBM, the current condition of the system is monitored to understand if the system is healthy, and, if not, to proceed for diagnosis. Fig 7 shows the comparison of the healthy mode with all eight fault modes for each feature selected to monitor the engine's current condition. These features are chosen because their profiles are distinct for every fault mode, making them easier to distinguish from the healthy profile and also to isolate the exact fault mode.

From fig 7, it can be clearly seen that the **Reduced Fuel flow** fault mode is far from the healthy profile in all four features, making it easy to detect. In other words, in this fault mode, reduction of the fuel flow rate by 10% leads to the engine running off-design, resulting in reduced core speed, pressures, and temperatures measured at the stations (fig 7) and reduced gross thrust (fig 6).

In fig 7(a) it can be observed that the fault modes **HPC Contamination** and **HPT Blade Broken** have lower core speed when compared to the healthy profile, whereas all the other fault modes have higher core speeds. This is because the core speed refers to the high pressure shaft speed, which connects HPT and HPC (from fig 4). Hence the loss of efficiency in either HPC or HPT would result in reduced core speed. However, in case of loss of efficiency in any other subsystem like the fan, LPC, or LPT, the high pressure shaft will run faster to obtain the demanded thrust, resulting in higher core speed when compared to the healthy profile.

In fig 7(b), which shows the profiles of LPC exit pressure, **Fan FOD**, **LPC fouling**, and **LPT Blade Broken** fault modes have pressures lower than the healthy pressure profile. The reason behind the difference is the low pressure shaft that connects fan, LPC, and LPT. Loss of efficiency in these subsystems, because of fouling, or the loss of material, leads to

lower intake of air resulting in lower compression developed by the LPC.

The opposite is true for **HPC contamination** and **HPT Blade Broken** fault modes. Here, the loss of efficiency in the HPC results in lower compression by the HPC, and loss of efficiency in the HPT results in the HPC being driven with a lower speed. Hence, there is slight pressure build up at the entrance of the HPC, as the HPC cannot compress to its fullest in both cases.

In fig 7(c), it can be observed that loss of efficiency of any subsystem in the engine results in higher turbine exhaust gas temperature because of the extra workload on the engine to achieve the demanded thrust. While fig 7(a), 7(b), and 7(c) showed a clear distinction between fault modes affecting the main subsystems of the engine, the fault modes **Bleed Valve Stuck**, and **Customer Discharge Pressure (CDP) leakage** are not seen clearly, as they have profiles similar to the healthy one. These two fault modes are distinguished only with the help of pressure measured at the exit of the bleed air duct, which in this instance shows a distinguishing profile for all the fault modes, as seen in 7(d).

Thus, with the help of these four features chosen by the mRMR algorithm, the current health state of the engine is monitored, and degradation in any of the subsystems can be easily detected by comparing their performance profile with that of the healthy profile. Therefore, the four features of the engine, viz, the core speed, Pt_S24, Tt_S5, and Pt_AfCDP together form the symptom vector for the engine diagnosis.

B. THE ENVIRONMENTAL CONTROL SYSTEM (ECS)

The Environmental Control System (ECS) of an aircraft maintains the in-flight conditions suitable for the passengers as well as for the effective functioning of the onboard equipment. The bleed air system (BAS) in the ECS receives bleed air extracted from the APU (on the ground) and the engine (during flight) and passes it to the anti-icing system and the PACK (passenger air conditioner). The PACK is the subsystem in the ECS responsible for conditioning the bleed air to be supplied to the cabin. The PACK consists of a series of components such as the primary heat exchanger (PHX), the secondary heat exchanger (SHX), air cycle machine (ACM), high pressure water separator (HPWS), temperature control valve (TCV), and a flow control valve called the Pack Valve (PV). The PACK conditions the pressure (P), temperature (T), and specific humidity (SH) of the bleed air to match the flight deck requirements. The conditioned air then passes through a mixed manifold system and air distribution system to the cabin, and the cabin pressure control system regulates the air pressure inside the cabin as required by the flight deck [26].

1) DIGITAL TWIN SETUP

In order to simulate the operation of the ECS, a simulation package called SESAC (Simscape Environmental control system Simulation under All Conditions) is chosen [26]. SESAC provides a library of components to perform simulation of the ECS under a wide range of operating conditions

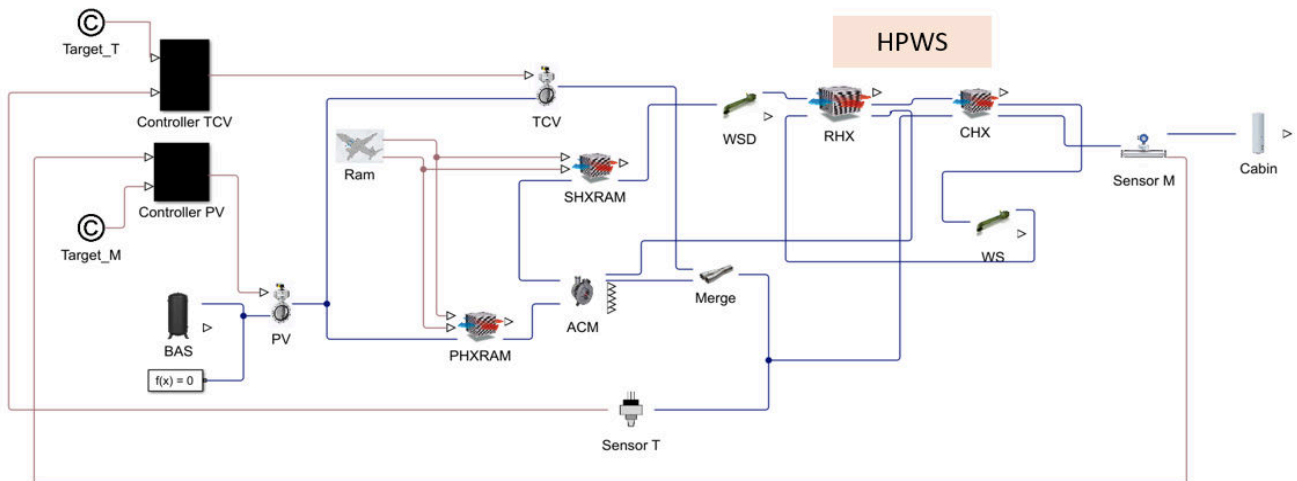


FIGURE 8. B737-800 ECS PACK model emulated in SESAC [26].

for both healthy and faulty scenarios. The SESAC component library has been configured to produce a detailed model of the B737-800 PACK. This model has been validated against actual data from the aircraft [26]. Fig 8 shows a schematic of the PACK model in SESAC. The bleed air from the engine or the APU is received at high temperature and pressure by the ECS. The PACK uses the PV to control the flow of this air, a portion of which is passed through the PHX for heat to be removed. This air is then cooled further by the compressor (as part of the ACM) and the SHX. Ram air is used by both heat exchangers (PHX and SHX) as a heat sink. The HPWS consists of a Reheater (RHX), condenser (CHX), and water separator (WS), which together remove any condensation from the air before it enters the turbine (the other ACM component). The cooled air is then merged with the bypassed hot air, the TCV regulating the flow as demanded. Further details on the PACK model in SESAC can be found in this reference [26].

For the work here, the digital twin is fed with input conditions of 28000 ft altitude and 0.761 Mach number to meet the target cabin pressure of 79.1kPa, cabin temperature of 291.24K, and mass flow rate of 0.445 kg/s. In order to develop diagnostics for the ECS, the simulation of a 100% healthy scenario is run in SESAC, followed by injection of six faults which are listed below, combining local and interacting faults as for the engine case.

Local Faults:

- i) **ACM 0.6:** only 60% mechanical efficiency of the ACM is simulated.
- ii) **PHX Fouling:** Fouling in the PHX, leading to its efficiency reduced by 50%.
- iii) **SHX Fouling:** Fouling in SHX, leading to 50% reduction in efficiency.

Interacting Faults:

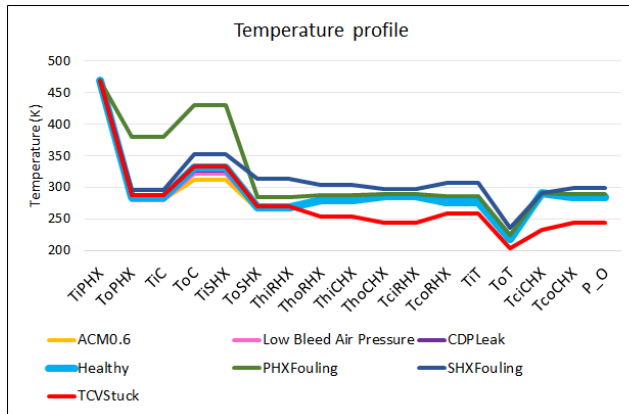
- iv) **CDP Leak:** this fault is due to 0.5% leakage in Customer Discharge Pressure (CDP) from the engine.

- v) **Low Bleed air Pressure:** this fault could be due to the HPSOV being stuck in the bleed air system, reducing the input bleed air to 75% of the original demand.
- vi) **TCV Stuck:** TCV is stuck at 10 degrees. This fault could be due to an intermittent supply from the EPS to the TCV.

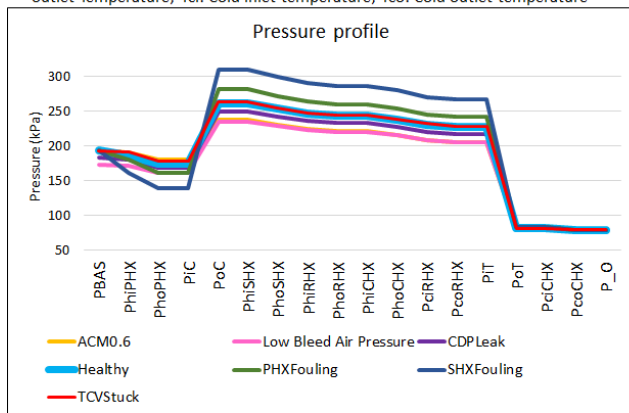
As in the case of the engine, the percentage loss of efficiency and leakage are chosen randomly, and hence these faults can be compared for trend, but cannot be quantitatively compared with each other. Temperature (T) and pressure (P) are measured at the inlet and outlet of every subsystem along the path of the bleed air.

Fig 9 (a) shows the temperature profile for the healthy and faulty simulation scenarios. The monitored parameters are laid out in the way that represents the path followed by bleed airflow in the PACK. In the healthy scenario (sky blue colour), the temperature of the bleed air is first reduced by passing it through PHX. It then increases slightly when compressed by the ACM compressor, after which the temperature decreases as the compressed air passes through the SHX. The air is reheated within the RHX and condensed in the CHX; hence the temperature increases in the hot sides of both RHX and CHX.

The air is sent through the water separator and again through the cold side of RHX, where the temperature remains constant. The air is expanded by the turbine, with the temperature reducing dramatically. This expansion work directly powers the compressor (on the same spool as the turbine). After this, the temperature of the expanded air increases when mixed with the hot airflow, to meet the cabin target temperature, before leaving the PACK outlet. Fig 9(b) shows the pressure profile, where, in the healthy scenario, the pressure of the bleed air decreases towards the PHX exit, followed by an increase in pressure when the air is compressed in the ACM. When the compressed air passes through the HPWS components (RHX and CHX), the pressure reduces gradually, followed by a dramatic reduction when the air is expanded



(a) Temperature profile of PACK for healthy and faulty scenarios (Ti: Inlet temperature; To: Outlet temperature; Thi: Hot inlet temperature; Tho: Hot outlet Temperature; Tci: Cold inlet temperature; Tco: Cold outlet temperature)



(b) Pressure profile of PACK for healthy and faulty scenarios (Pi: Inlet pressure; Po: Outlet pressure; Phi: Hot inlet pressure; Pho: Hot outlet pressure; Pci: Cold inlet pressure; Pco: Cold outlet pressure)

FIGURE 9. Temperature and pressure profiles for healthy and faulty scenarios for ECS PACK simulation in SESAC.

through the turbine. This pressure is maintained as the air passes towards the PACK outlet.

Fault mode *ACM 0.6*, reducing the mechanical efficiency of the ACM, gives a lower temperature (fig 9(a)) and pressure (fig 9(b)) output from the compressor relative to the healthy case.

Fault modes *PHX Fouling* and *SHX Fouling* lead to less heat exchanged when air passes through the corresponding heat exchangers, resulting in higher temperatures at their outlets, as seen in fig 9(a). However, the effect of degradation in PHX is negated by SHX, but the effect of degradation in SHX is carried forward into the HPWS, resulting in a higher turbine inlet temperature. Therefore, the pressure ratio increases between the turbine and the compressor, as seen in the pressure profile for *SHX Fouling* (fig 9(b)).

Fault modes *CDP Leak* and *Low Bleed air Pressure* allow air at lower pressure inside the PACK; hence, they are characterised by lower temperature and pressure profiles, similar to *ACM0.6*.

In the *TCV Stuck* fault mode, when the temperature control valve is stuck at 10 degrees, it only allows air at a lower mass

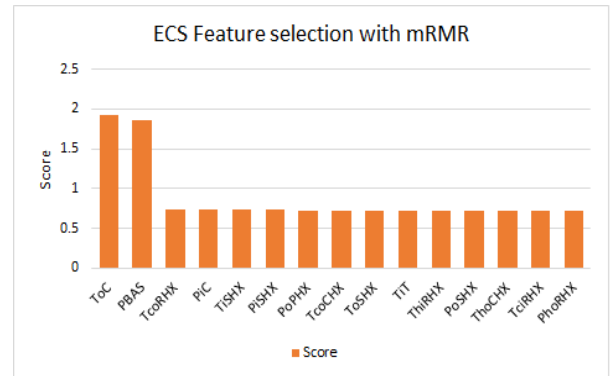


FIGURE 10. mRMR algorithm for the ECS features selection.

flow rate to pass. Hence the remaining air is cooled down much more than it should be, as seen in fig 9(a), and pressure profile is slightly higher than the healthy case.

While all six fault modes have individualistic profiles when compared to the healthy profile, monitoring all 32 parameters to detect the current state of the ECS would be tedious, time-consuming and consume more computational power. Hence, feature selection is used, similar to the case of the engine, to choose only the most relevant parameters to the response variable.

2) DATA ACQUISITION AND DATA MANIPULATION

The ECS digital twin is run in MATLAB R2019b for both healthy and faulty scenarios. For the ECS model in SESAC, temperature and pressure parameters are monitored at the inlet and exit of all ECS subsystems along its path. Using the mRMR algorithm explained in Section III (A.2), the 34 monitored features are ranked and scored. The features with the first 15 scores are shown in fig 10. The first two features have higher scores, followed by a large drop in the scores for the other features. This drop signifies the confidence level of the scores of the first two features, implying that, they are better predictors of ECS health. Hence, the final list of four features chosen from fig 10 for the condition monitoring and diagnosis of the ECS are i) Outlet temperature of the compressor (ToC), ii) pressure from the bleed air system (PBAS), iii) Reheater cold side outlet temperature (TcoRHX), and iv) Compressor inlet pressure (PiC).

3) STATE DETECTION

Instead of monitoring all 34 parameters listed in fig 10, the current condition of the ECS will be detected by monitoring only the four parameters chosen by the mRMR algorithm, as shown in fig 11. It can be seen from fig 11 that each chosen feature is able to distinguish more than one faulty scenario from the healthy profile. For example, from fig 11(a), ToC has a distinguished profile for *PHX Fouling*, *SHX Fouling*, and *ACM 0.6*. Fig 11(b) shows the differences between *Low Bleed air Pressure* and *CDP Leak*. Fig 11(c) has a clear difference between *PHX Fouling*, *SHX Fouling*, *TCV Stuck*, and the healthy scenario, and fig 11(d) shows a distinction

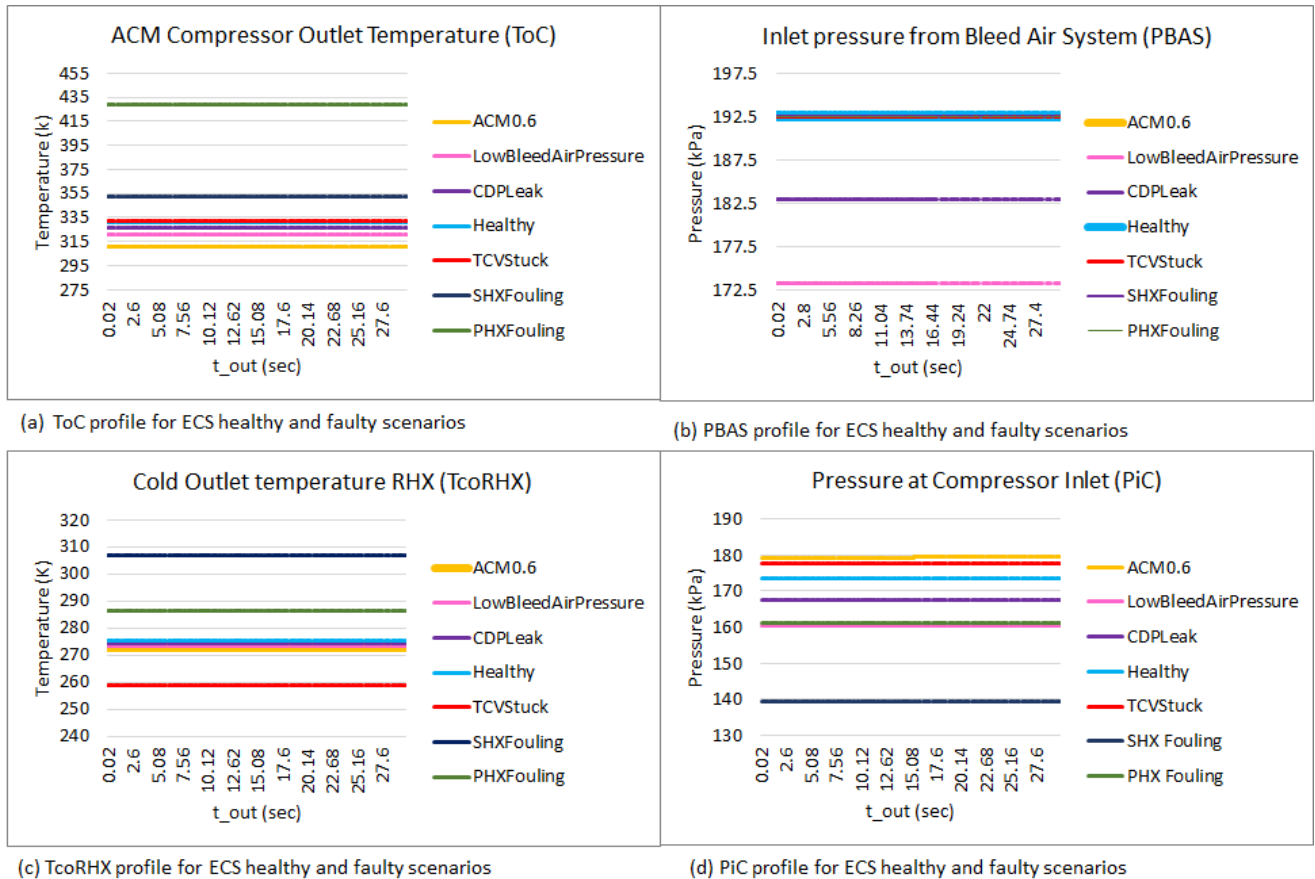


FIGURE 11. Healthy and faulty case profiles for ECS features selected by mRMR algorithm.

between most of the faulty scenarios. Using a combination of these four features alone will be sufficient to detect the presence of a fault in the ECS. Hence, the features ToC, PBAS, TcoRHX, and PiC form the symptom vector for the ECS to carry out the required diagnosis.

C. THE FUEL SYSTEM

The primary function of the fuel system is to supply fuel to the engine and APU at the required pressure and temperature. In a typical twin-engine aircraft, the fuel system has three tanks, two in the wings and one at the centre of the fuselage. Both the engines consume fuel, at pressure, from the centre tank until it reaches a low level, and then they use fuel from their respective main tanks. The fuel system transfers fuel from the tank through the first stage fuel pump, the fuel oil heat exchanger, fuel filter, and then to the second stage boost pump. Fuel flow is then measured, after which the fuel enters the manifold and is supplied to the combustion chamber in the engine. Since the primary function of the fuel system depends upon the fuel transfer lines, any failure in these components could result in safety issues. The possibility of faults like pump failures, leakage in the fuel pipes, clogging in the filters, sticking valves, and blockages are taken care of during maintenance in order to prevent their occurrence

in flight. There are several diagnostic methods developed to isolate faults to the LRU level to help with troubleshooting activities [27]–[30].

1) EXPERIMENTAL SETUP

The fuel system is represented by an experimental setup in the IVHM Centre’s laboratory and is therefore treated as HIL [31]. A simulation could have been written and used as in the previous two examples, but the use of a rig for this example serves to show the flexibility of the overall approach. The fuel rig shown in fig 12 is a closed loop, where fuel (water) is pumped from a reservoir R by a motor driven pump P that has an internal relief valve, passing through a shut off valve S, followed by another valve V, a filter F, flowmeters FM1, FM2, a nozzle N and back to the reservoir R.

The control system is programmed using LabView software, and the experiments are run at a constant flow rate or constant pump speed. The speed of the motor driven pump on the test rig is controlled by LabView to meet with the required flow rate or a selected pump speed. Filters, valves, and nozzles on the test rig are emulated by Direct acting Proportional Valves (DPV), which are also controlled with LabView. Faults are injected, at different severity levels, by controlling the opening rates of these DPVs. Pressure sensors

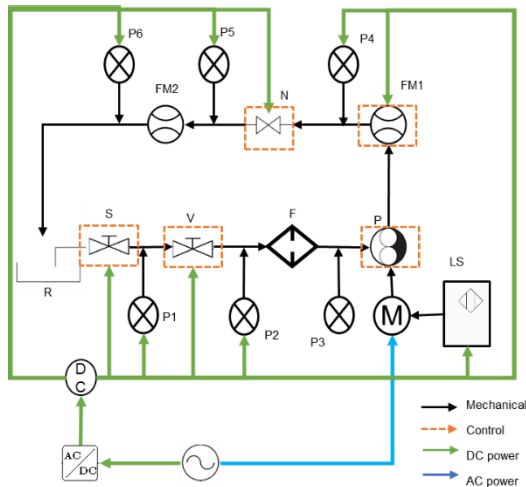


FIGURE 12. Layout of the fuel rig setup in IVHM centre.

P1, P2 . . . , P6, are installed to monitor the pressure along the line, and they are powered by 12.8 VDC power supply. The laser sensor L, which is used for measuring the pump speed, is powered by 10-30VDC. The pump motor is powered by three phase 230/400 VAC at 50 Hz [31].

With the above-mentioned arrangement, the following five faults are injected into the fuel rig.

Local Faults:

- i) **Sticking Valve:** Fault injected by manipulating the valve V by changing the opening rate of DPV from 100% to 90%, 80%, 70%, and 60%, emulating 0% severity of degradation to 10%, 20%, 30%, and 40% respectively.
- ii) **Clogged Filter:** Fault injected by manipulating the filter F by introducing severity in increments of 10%, up to 40% degradation.
- iii) **Clogged Nozzle:** Fault injected by manipulating the Nozzle N by introducing severity in increments of 10% up to 40% degradation.
- iv) **Blocked Flow Meter:** Fault injected by blocking the flow meter FM1 by introducing severity in increments of 10% up to 40% degradation.

Interacting Fault:

- v) **Reduced flow:** Fault simulated by reducing the pump speed, because of low voltage supplied to the pump motor M. This is considered as an interacting fault, due to the involvement of the EPS in supplying reduced voltage to the pump motor.

With the pressure sensors, along with pump speeds, being monitored, the fuel rig is first run at the 100% healthy condition at a constant flow rate of 0.5 litre per minute (lpm), at the beginning of every experiment. The results from running at this condition are, as might be expected, highly repeatable. The health of components is reduced gradually from 100% to 90%, 80%, 70%, and 60% subsequently by manipulating the DPVs, giving a block of experiments for each failure mode.

2) DATA ACQUISITION AND DATA MANIPULATION

For the fuel system, all experiments are initially run at the healthy condition, followed by fault injection. Readings from the sensors in the fuel rig are collected at a frequency of 1 kHz. [31]. The data is collected from the LABVIEW environment as.lvm files, which are then converted to.csv files and processed into MS EXCEL for further analysis.

In the fuel rig experiment, there are only six pressure sensors and a laser sensor for measuring pump motor speed. Hence, due to the low number of possible features, the mRMR algorithm is not applied here, and all seven parameters are chosen for state detection and diagnosis.

3) STATE DETECTION

Fig 13 shows the pressure profiles and pump speed variation during each fault mode while trying to maintain the constant fuel flow objective.

Fig 13(a) shows the pressure profile for fault mode **Sticking Valve**, the pressure values at P2 and P3 decrease with increase in the fault severity. This is consistent with the fault being injected in the valve (V) that lies between pressure sensors P1 and P2. The fault results in an increased pressure drop across the valve, and since the fuel rig is controlled to run for constant flow, the pressure drop continues to be observed up to P3. Since the motor pump is controlled to meet the constant flow of 0.5 lpm, the pump speed increases with the increase in severity of the fault, as seen in fig 13(b). The values of P4, P5, and P6 do not change since the pump, delivering a constant mass flow, shields them.

Fig 13(c) shows the pressure profile and fig 13(d) the pump speed profile, for a constant flow rate during **Clogged Filter**. There is an increase in pressure drop between P2 and P3 as the filter is located between these two sensors. The pressure values at other locations remain the same. The pump speed increase with the severity of degradation to meet with the constant flow demand, as observed in fig 13(d).

Fig 13(e) shows the pressure profile and pump speeds for **Clogged Nozzle**. The nozzle N is located after the pump between P4 and P5, as shown in fig 12. When this fault is injected pressure increases at P4, just before the nozzle location. The rest of the pressure sensor readings remain the same. It can be seen from fig 13(f) that the pump speed increases rapidly to meet the constant flow rate demand.

When the **Blocked flowmeter** fault is injected (fig 13(g)), it generates a back pressure to the motor pump, and the pump speed increases to maintain the flow at 0.5 lpm as observed in fig 13(h). There is no pressure sensor between the pump and the flowmeter, and hence the pressure profile does not indicate any change when this fault is injected.

In the case of the **Reduced Flow** fault mode the pump speed was reduced by 50 rpm per experiment, starting from 400 rpm to 250 rpm, to emulate the reduced flow in the line. The response of all pressure sensors is seen through the gradual change, as observed in fig 13(i), with respect to change in the

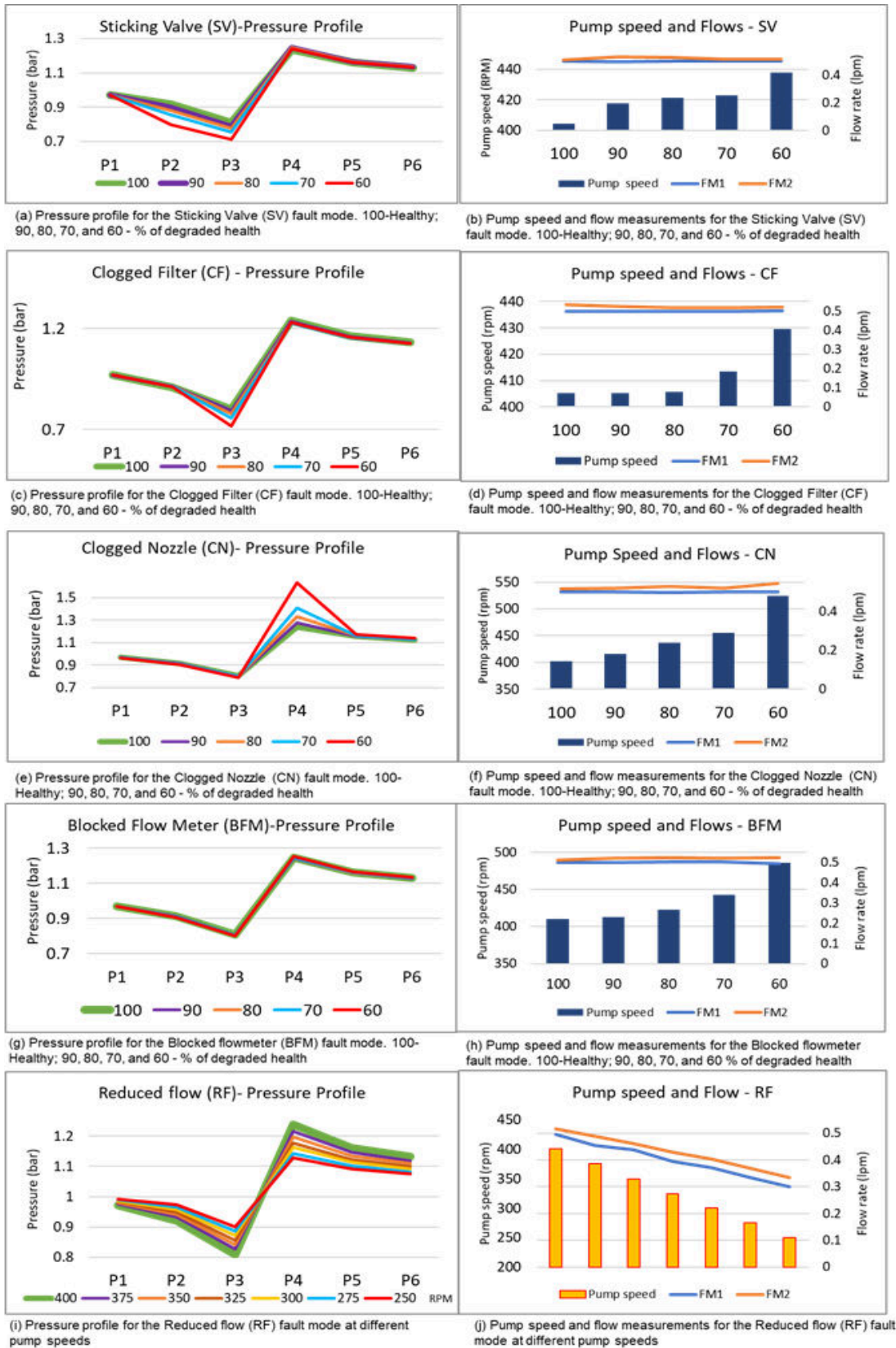


FIGURE 13. Pressure profiles, pump speeds and flows for various faulty scenarios from fuel rig experiment.

pump speed. The change in flow rate with respect to the pump speed, as shown in fig 13(j).

Thus, the seven parameters (P1, P2, . . . , P6, Pump Speed) from the fuel rig experiment form the features for the symptom vector for the diagnosis of faults in the fuel rig.

IV. DIAGNOSIS

Once the features have been shortlisted for being candidates for the symptom vector for each system, the next step in the OSA-CBM methodology is diagnosis.

In this article, diagnosis is treated as a multi-class classification problem, in which, the symptom vector is classified as belonging to any of the fault class or labelled as healthy. In order to devise the diagnostics for all three aircraft systems, the data collected from the experiments are trained with machine learning classification algorithms and tested for their accuracy of classification. It is to be noted that the model-based diagnosis can also be implemented using the OSA-CBM methodology. However, they are not tested in this article, and only data-driven diagnosis is implemented for creating uniformity in developing similar diagnostic functions for different aircraft systems.

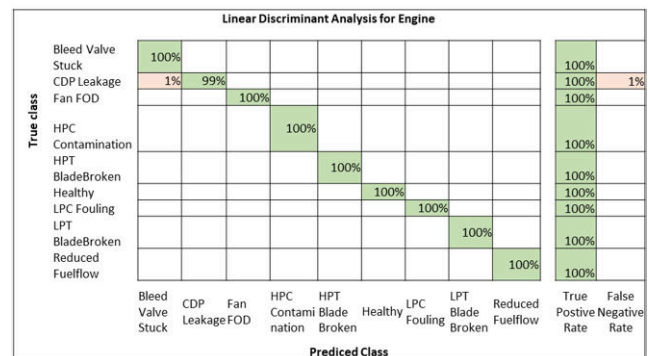
Data from the chosen features from each use case is collected and split into training and testing datasets by Monte-Carlo simulation at 60%-40%, respectively. The datasets for training are uploaded into the MATLAB Classification Learner application and trained using various classification algorithms.

The training uses various supervised machine learning algorithms in this multi-class classification problem, and the best performer is chosen for the next stage. The algorithms chosen for comparison are Decision trees, k-Nearest Neighbor (kNN), Linear Discriminant Analysis (LDA), and Support Vector Machines (SVM). While the decision tree algorithm classifies the symptom vector based on rules and conditions developed using the training sets, the kNN algorithm assigns value to the symptom vector and classifies based on how its points are when compared to the training set. The LDA algorithm calculates the means and covariance matrix for different classes from the training set and classifies the symptom vector based on its computed values. In the SVM method, hyperplanes are created based on the classes from the training set. The symptom vectors are assigned co-ordinates and are classified based on their distances from the hyperplanes. The mathematics behind these algorithms can be found in these references [32], [33], and are not discussed in this article. Datasets from each aircraft system are trained using all four algorithms and are tested for their accuracy of classification.

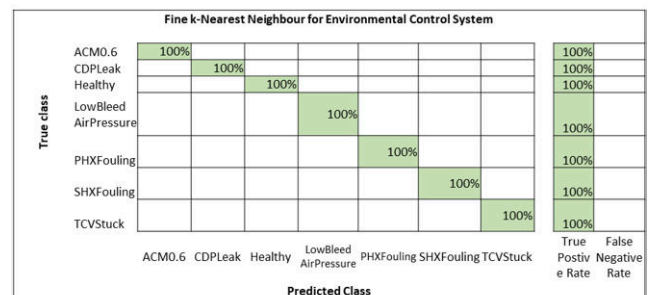
Table 1 shows the accuracy in classification, i.e., in diagnosing fault modes, using the machine learning algorithms, for each of the aircraft system use cases outlined in this article. It appears from the table, and judicious choice of features, that any of these algorithms could be used to diagnose faults to quite high levels.

TABLE 1. Accuracy of Classification by Machine Learning Algorithms for the Diagnosis of Faults in Three Aircraft Systems.

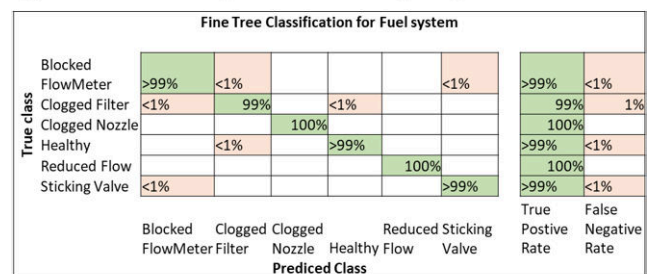
	Engine	Environmental Control System	Fuel System
Decision Tree	93.2%	100%	99%
k-Nearest Neighbour	99.1%	100%	88.9%
Linear Discriminant Analysis	99.9%	100%	89.2%
Support Vector Machines	99.8%	100%	95.1%



(a) Confusion Matrix for Engine diagnosis with Linear Discriminant Analysis



(b) Confusion Matrix for ECS diagnosis with Fine k-Nearest Neighbor Algorithm



(c) Confusion Matrix for Fuel System diagnosis with Fine Decision Tree Algorithm

FIGURE 14. Confusion matrices for best classification method for three aircraft systems.

The LDA algorithm is chosen for the engine diagnostics, as it shows 99.9% classification accuracy. For the ECS, all four algorithms show 100% classification accuracy, and the kNN algorithm is chosen for the ECS diagnostics for its ease of computation compared to the other algorithms. The decision tree algorithm is chosen for the fuel system

TABLE 2. Summary of the Use Cases Demonstrated Using OSA-CBM Methodology.

OSA-CBM Steps	Engine	Environmental Control System	Fuel System
Digital twin Simulation Platform	T-MATS	SESAC	Test rig in IVHM Centre
No. of Fault modes	8	6	4 fault modes with 4 degradation levels + 1 fault mode with 7 degradation levels
Data Acquisition and Manipulation	85 features monitored	34 features monitored	7 features monitored
State detection	With 4 chosen features	With 4 chosen features	With 7 chosen features
Health Assessment (Diagnosis algorithm)	Linear Discriminant Analysis	k-Nearest Neighbour	Decision Tree

diagnostics for having 99% accuracy from table 1. Fig 14 shows the confusion matrix for the best methods for each of these aircraft systems.

The better performer in each use case is chosen for the next stage, depending upon the application in which the diagnostic results are used. For example, if the diagnostic results are used in aircraft maintenance directly, they can be helpful in troubleshooting and fault isolation. On the other hand, these diagnostic results could also be used for remaining useful life calculations in the prognostic step of OSA-CBM methodology, followed by the advisory generation step, which is to develop suitable maintenance plans for the particular aircraft system. In FAVER, these diagnostic results will be used in the next stage of this research work for further reasoning at the vehicle level to identify cascading faults and root causes.

V. SUMMARY AND FUTURE WORK

In this article, the OSA-CBM methodology has been used to demonstrate the process of developing system level diagnostics for multiple aircraft systems. Table 2 presents a summary of the use cases demonstrated in this article. In order to emulate a typical industrial scenario, the digital twin of each aircraft system has been developed separately and is isolated from the others. They have various faults injected, some affecting the local system, and some interacting with other systems. They have a different number of features monitored for assessing the health of the systems. Developing diagnostics for such independent aircraft systems is generally time-consuming. However, the application of the OSA-CBM methodology has helped in establishing uniformity in building the system level diagnostics into the framework. The developed diagnostic functions in MATLAB can isolate a certain number of faults, with just a few chosen monitored features. These features form a symptom vector for each of the targeted aircraft systems.

While this article demonstrated how the bottom three layers from FAVER's schematic in fig 1 (starting from the digital twin layer to the diagnosis layer) are brought together, the future work will present how FAVER uses the symptom vectors generated from these aircraft systems to isolate faults and their root causes. These papers will also discuss the

architecture of FAVER, the reasoning mechanism involved, and demonstration of isolation of faults and identification of the root causes and their cascading effects on interacting aircraft systems.

LIST OF ABBREVIATIONS

ACM	Air Cycle Machine
APU	Auxiliary Power Unit
CDP	Customer Discharge Pressure
CHX	Condensor
DPV	Direct acting Proportional Valves
ECS	Environmental Control System
EPS	Electrical Power System
FAA	Federal Aviation Administration
FAVER	A Framework for Aerospace Vehicle Reasoning
FOD	Foreign Object Damage
HIL	Hardware-in-the-loop
HPC	High Pressure Compressor
HPT	High Pressure Turbine
HPWS	High Pressure Water Separator
IVHM	Integrated Vehicle Health Management
kNN	k-Nearest Neighbour
LDA	Linear Discriminant Analysis
LPC	Low Pressure Compressor
LPT	Low Pressure Turbine
LRU	Line Replaceable Unit
MI	Mutual Information
MIQ	Mutual Information Quotient
mRMR	minimum Redundancy Maximum Relevancy
MRO	Maintenance, Repair, and Overhaul
OEM	Original Equipment Manufacturer
OSA-CBM	Open Standard Architecture for Condition Based Maintenance
PACK	Passenger air conditioner
PBAS	pressure from the bleed air system
PHX	Primary Heat Exchanger
PiC	Compressor inlet pressure
Pt_AfCDP	Pressure at the exit of bleed air duct
Pt_S24	Pressure at LPC exit (station 24)

RHX	Reheater
SESAC	Simscape Environmental control system Simulation under All Conditions
SHX	Secondary Heat Exchanger
SVM	Support Vector Machine
TcoRHX	Reheater cold side outlet temperature
TCV	Temperature Control Valve
TFSC	Thrust Specific Fuel Consumption
T-MATS	Toolbox for Modeling and Analysis of Thermodynamic Systems
ToC	Outlet temperature of the compressor
Tt_S5	Temperature at LPT exit (station 5)

ACKNOWLEDGMENT

The authors would like to thank Dr. Fakhre Ali and Dr. Christos Skliros for their help in setting up the digital twins for the ECS and the engine. The authors would like to thank Boeing for their support of this project.

REFERENCES

- [1] Mike Monroney Aeronautical Center, Federal Aviation Administration. (2008). *Federal Aviation Administration Joint Aircraft System/Component Code and Table Definitions*. Accessed: Sep. 12, 2020. [Online]. Available: https://av-info.faa.gov/sdrx/documents/JASC_Code.pdf
- [2] C. M. Ezhilarasu, Z. Skaf, and I. K. Jennions, "Progress towards a framework for aerospace vehicle reasoning (FAVER)," in *Proc. Annu. Conf. PHM Soc.*, 2019, vol. 11, no. 1, pp. 1–9.
- [3] C. M. Ezhilarasu, Z. Skaf, and I. K. Jennions, "Understanding the role of a digital twin in integrated vehicle health management (IVHM)," in *IEEE Int. Conf. Syst., Man Cybern. (SMC)*, Oct. 2019, pp. 1484–1491.
- [4] S. Vohnout, B. Kim, N. Kunst, B. Gleeson, R. Wagoner, E. Balaban, and K. Goebel, "A model-based avionic prognostic reasoner (MAPR)," in *Proc. Infotech@Aerospace*, 2012, pp. 1–17.
- [5] M. Watson, J. Sheldon, S. Amin, H. Lee, C. Byington, and M. Begin, "A comprehensive high frequency vibration monitoring system for incipient fault detection and isolation of gears, bearings and shafts/couplings in turbine engines and accessories," in *Proc. Turbo Expo*, vol. 5, 2007, pp. 885–894.
- [6] S. Sarkar, D. S. Singh, A. Srivastav, and A. Ray, "Semantic sensor fusion for fault diagnosis in aircraft gas turbine engines," in *Proc. Amer. Control Conf.*, Jun. 2011, pp. 220–225.
- [7] C. M. Ezhilarasu, Z. Skaf, and I. K. Jennions, "The application of reasoning to aerospace integrated vehicle health management (IVHM): Challenges and opportunities," *Prog. Aerosp. Sci.*, vol. 105, pp. 60–73, Feb. 2019.
- [8] Mimos. (2010). *OSA-CBM UML Specification 3.3.1 Release, Machine Information Management Open Systems Alliance*. Accessed: Sep. 12, 2020. [Online]. Available: <https://www.mimos.org/specifications/osa-cbm-3-3-1/>
- [9] *Condition Monitoring and Diagnostics of Machines*, document ISO 13374, International Organization for Standardization, 2015.
- [10] T. Sreenuch, A. Tsourdos, and I. K. Jennions, "Software framework for prototyping embedded integrated vehicle health management applications," *J. Aerosp. Inf. Syst.*, vol. 11, no. 2, pp. 82–97, Feb. 2014.
- [11] J. Dunsdon and M. Harrington, "The application of open system architecture for condition based maintenance to complete IVHM," in *Proc. IEEE Aerosp. Conf.*, vol. 4, Mar. 2008, pp. 1–9.
- [12] K. Keller, A. Del Amo, and B. Jordan, "Aircraft electrical power systems prognostics and health management (AEPHM)," SAE Tech. Paper 2004-01-3162, 2004.
- [13] G. Bastard, J. Lacaille, J. Coupard, and Y. Stouky, "Engine health management in safran aircraft engines," in *Proc. Annu. Conf. Prognostics Health Manage. Soc. (PHM)*, Oct. 2016, pp. 101–108.
- [14] V. N. Divakaran, R. M. Subrahmanya, and G. V. V. Ravikumar. (2018). *White Paper Integrated Vehicle Health Management of a Transport*. Infosys. Accessed: Jan. 1, 2021. [Online]. Available: <https://www.infosys.com/engineering-services/white-papers/Documents/aircraft-landing-gear-system.pdf>
- [15] W. Bense, "Prognosis and health monitoring systems for aircraft engines," in *Proc. SAE Int., SAE AeroTech Congr. Exhib.*, 2013, p. 8, doi: 10.4271/2013-01-2146.
- [16] J. Du, S. Wang, L. Han, S. Zhao, and C. Guo, "Prognostic management verification system of aircraft hydraulic power supply system," in *Proc. IEEE 10th Int. Conf. Ind. Informat.*, Jul. 2012, pp. 693–699.
- [17] C. M. Ezhilarasu and I. K. Jennions, "A system-level failure propagation detectability using ANFIS for an aircraft electrical power system," *Appl. Sci.*, vol. 10, no. 8, p. 2854, Apr. 2020.
- [18] NASA Glenn Research Center. *How Does a Jet Engine Work?* Accessed: Jan. 16, 2018. [Online]. Available: <https://www.grc.nasa.gov/www/k-12/UEET/StudentSite/engines.html>
- [19] J. W. Chapman, T. M. Lavelle, R. D. May, J. S. Litt, and T. Guo, "T-MATS: Toolbox for the modeling and analysis of thermodynamic systems user's guide," Glenn Res. Centre, Cleveland, OH, USA, Tech. Rep. NASA/TM—2014-216638, 2014, p. 50. [Online]. Available: <https://ntrs.nasa.gov/api/citations/20140012486/downloads/20140012486.pdf>
- [20] J. W. Chapman, T. M. Lavelle, J. S. Litt, and T. Guo, "A process for the creation of T-MATS propulsion system models from NPSS data," in *Proc. 50th AIAA/ASME/SAE/ASEE Joint Propuls. Conf.*, 2014, p. 3931.
- [21] H. Peng, F. Long, and C. Ding, "Feature selection based on mutual information criteria of max-dependency, max-relevance, and min-redundancy," *IEEE Trans. Pattern Anal. Mach. Intell.*, vol. 27, no. 8, pp. 1226–1238, Aug. 2005.
- [22] Mathworks. *Fscmmr*. Accessed: Jul. 8, 2020. [Online]. Available: https://www.mathworks.com/help/stats/fscmmr.html#mw_bacedbf4-b0ee-4a43-97ee-5de3f6696e6a
- [23] S. Garg, "Fundamentals of aircraft turbine engine control," Glenn Res. Centre (NASA), Lewis Field, Cleveland, OH, USA, 2015. [Online]. Available: https://www.grc.nasa.gov/WWW/cdt/aboutus/Fundamentals_of_Engine_Control.pdf
- [24] . Yılmaz, "Evaluation of the relationship between exhaust gas temperature and operational parameters in CFM56-7B engines," *Proc. Inst. Mech. Eng., G, J. Aerosp. Eng.*, vol. 223, no. 4, pp. 433–440, Apr. 2009.
- [25] M. T. Yildirim and B. Kurt, "Aircraft gas turbine engine health monitoring system by real flight data," *Int. J. Aerosp. Eng.*, vol. 2018, no. 1, p. 12, 2018.
- [26] I. Jennions, F. Ali, M. E. Miguez, and I. C. Escobar, "Simulation of an aircraft environmental control system," *Appl. Thermal Eng.*, vol. 172, Nov. 2019, Art. no. 114925.
- [27] E. M. Kelly and L. M. Bartlett, "Aircraft fuel rig system fault diagnostics based on the application of digraphs," *Proc. Inst. Mech. Eng., O, J. Risk Rel.*, vol. 221, no. 4, pp. 275–284, Dec. 2007.
- [28] S. C. Ofstun and S. Abdelwahed, "Practical applications of timed failure propagation graphs for vehicle diagnosis," in *Proc. IEEE Autotestcon*, Sep. 2007, pp. 250–259.
- [29] N. A. Snooke and M. H. Lee, "Qualitative order of magnitude energy-flow-based failure modes and effects analysis," *J. Artif. Intell. Res.*, vol. 46, pp. 413–447, Mar. 2013.
- [30] B. Lamoureux, J. Massé, and N. Mechbal, "An approach to the health monitoring of a pumping unit in an aircraft engine fuel system," in *Proc. Eur. Conf. Prognostics Health Manage. Soc.*, 2012, pp. 1–7.
- [31] Y. Lin, "System diagnosis using a Bayesian method," Ph.D. dissertation, Cranfield Univ., Cranfield, U.K., 2017.
- [32] M. Jung, O. Niculita, and Z. Skaf, "Comparison of different classification algorithms for fault detection and fault isolation in complex systems," *Procedia Manuf.*, vol. 19, pp. 111–118, Jan. 2018.
- [33] MathWorks. (2020). *Discriminant Analysis Classification*. Accessed: Aug. 1, 2020. [Online]. Available: <https://www.mathworks.com/help/stats/discriminant-analysis.html>



CORDELIA EZHILARASU received the bachelor's degree in aeronautical engineering and the master's degree in industrial engineering from Anna University, Chennai, India, in 2011 and 2013, respectively. She is currently pursuing the Ph.D. degree with Cranfield University. She was a Data Analysis Engineer with Bloom Energy and also a Senior Industrial Engineer with Lam Research for a period of 4 years. She has been with the IVHM Centre, since 2017. In her role as an Industrial engineer, she has worked on various process improvement projects and developed several semi-automated tools that contributed to time and cost savings for the organisation. Cordelia is a recognized ASQ Certified Six Sigma Black Belt. Her current research interests include IVHM technologies, digital twin, and machine learning related to aerospace applications.



ZAKWAN SKAF received the B.S. degree from the Faculty of Mechanical Engineering, in 2001, and the M.Sc. and Ph.D. degrees from the Control Systems Centre, University of Manchester, Manchester. He held several positions with Loughborough University, Sheffield University, Warwick University, and the University of Manchester. He is currently a Lecturer in diagnostics and prognostics with the Integrated Vehicle Health Management (IVHM), Cranfield University. He is an active researcher with more than 35 publications in many world-class peer-reviewed journals and conferences. His research interests include control engineering, data analytics, machine learning, condition monitoring, diagnostics, and prognostics related to aerospace, railway, marine, energy, and automotive applications.



IAN K. JENNIONS received the degree in mechanical engineering and the Ph.D. degree in CFD from Imperial College London, London. In July 2008, he was moved to Cranfield University as a Professor and the Director of the newly formed IVHM Centre. His career spans more than 40 years, working mostly for a variety of gas turbine companies. He has worked for Rolls-Royce (twice), General Electric and Alstom in a number of technical roles, gaining experience in aerodynamics, heat transfer, fluid systems, mechanical design, combustion, services, and IVHM. He is on the Editorial Board for the *International Journal of Condition Monitoring*, the Director of the PHM Society, the Chairman of SAE's IVHM Steering Group, a Contributing Member of the SAE HM-1 IVHM Committee, a Chartered Engineer, and a Fellow of IMechE, RAeS, and ASME. He is the editor of five SAE books and coauthored of another one.

• • •

2021-01-11

A generalised methodology for the diagnosis of aircraft systems

Ezhilarasu, Cordelia Mattuvarkuzhali

IEEE

Ezhilarasu CM, Skaf Z, Jennions IK. (2021) A generalised methodology for the diagnosis of aircraft systems. IEEE Access, Volume 9, 2021, pp. 11437-11454

<https://doi.org/10.1109/ACCESS.2021.3050877>

Downloaded from Cranfield Library Services E-Repository